Electroexcitation of low-lying states in ^{19}F

M. Oyamada, T. Terasawa, and K. Nakahara
Laboratory of Nuclear Science, Tohoku University, Tomizawa, Sendai 982, Japan

Y. Endo,* H. Saito, and E. Tanaka
Department of Physics, Tohoku University, Katahira, Sendai 980, Japan

(Received 20 January 1975)

Strong $E2$, $E3$, $E4$, and $E5$ excitations of low-lying states in ^{19}F were observed in an electron scattering experiment. From the measured form factors the following radiative transition strengths to the ground state (in Weisskopf units) were extracted: $|M(E2)|^2 = 8.1 \pm 1.0$ (the 1.55-MeV $\frac{3}{2}^+$ state), 1.0 ± 0.2 (4.56-MeV $\frac{5}{2}^+$); $|M(E3)|^2 = 11 \pm 3$ (1.35-MeV $\frac{5}{2}^-$), 15 ± 4 (5.43-MeV $\frac{7}{2}^-$); $|M(E4)|^2 = 5.8 \pm 1.3$ (2.78-MeV $\frac{9}{2}^+$); and $|M(E5)|^2 = 16 \pm 7$ (4.03-MeV $\frac{9}{2}^-$). A fairly large transverse form factor was found for the 2.78-MeV $\frac{9}{2}^+$ state. The value of $B(M5, \frac{9}{2}^+ \rightarrow \text{g.s.}) = (3.0 \pm 1.2) \times 10^4$ $e^2\,\text{fm}^{10}$ was extracted from the experimental data on the assumption that this transverse form factor resulted from $M5$ excitation only. The experimental form factors and radiative transition strengths for positive-parity states are compared with theoretical values calculated using the rotation-particle coupling (RPC) model; good agreement is obtained for the states predominantly belonging to the ground-state band: the 0.197-MeV $\frac{5}{2}^+$, 1.55-MeV $\frac{3}{2}^+$, and 2.78-MeV $\frac{9}{2}^+$ states. It is found that RPC is essential, in particular, to the $E4$ and $M5$ transitions of the 2.78-MeV $\frac{9}{2}^+$ state. The $E3$ transition strength of the 5.43-MeV $\frac{7}{2}^-$ state, as well as the 1.35-MeV $\frac{5}{2}^-$ state, is comparable with that of the octupole-vibrational state at 6.13 MeV in ^{16}O.

NUCLEAR REACTIONS ^{19}F(e, e'), $E = 134.5$, 150, 250 MeV; measured $\sigma(E; \theta)$; deduced $B(\Lambda)$. $(CF_2)_n$ target. Compared with the rotation-particle coupling model.

I. INTRODUCTION

The experimental studies of electromagnetic structures of low-lying states in ^{19}F have been extensively performed using various reactions by many authors.[1-11] The low-lying positive-parity states have been interpreted in terms of rotational bands.[12,13] The ground-state band of ^{19}F is generally believed to have a prolate deformation, because the sign of the quadrupole moment of the 0.197-MeV $\frac{5}{2}^+$ state is experimentally known to be negative.[1] The energy levels and strengths of $E2$ transitions within the ground-state band have been well explained not only in the rotational model but also in the shell model.[14-16] The higher multipole structures, however, have been less well investigated in both experiment and theory.

In the mass-number region $A = 18 \sim 28$, the strength of the $E2$ transition from the lowest collective quadrupole state to the ground state varies slowly as mass number increases, while the change in the $E4$ strength varies drastically, as is seen from experiments[17-19] on ^{20}Ne, ^{21}Ne, ^{24}Mg, and ^{28}Si. This drastic change in the $E4$ strength suggests that information on the hexadecapole structure may give a useful viewpoint from which one can understand features of the electromagnetic properties particular to each nuclide in the sd-shell region.

de Swiniarski *et al.*[19] have recently obtained a large hexadecapole deformation parameter $\beta_4 = 0.14$ of the optical potential from a coupled-channels analysis of proton scattering data on the ground-state rotational band: the ground $\frac{1}{2}^+$, 0.20-MeV $\frac{5}{2}^+$, 1.55-MeV $\frac{3}{2}^+$, and 2.78-MeV $\frac{9}{2}^+$ states. This value of β_4 is one-half of that for ^{20}Ne obtained from the same analysis. As pointed out by Paul,[12] however, band mixing is important in the low-lying states in ^{19}F because of strong rotation-particle coupling (RPC) caused by the Coriolis force. Therefore the validity of the rotational model with and without band mixing can be checked for the hexadecapole transition. This point affects the simple comparison of the values of β_4 mentioned above in the sense of the nuclear surface deformation.

On the other hand, negative-parity states have somewhat different features. It is well known that the low-lying negative-parity states in ^{19}F are strongly excited by α-particle transfer reactions on ^{15}N,[20] and exhibit very strong $E2$ transitions.[1] These properties have been well explained in terms of the weak-coupling model,[21] in which a negative-parity band of ^{19}F is formed by weak coupling of a $1p_{1/2}$ proton hole to the ground-state band of ^{20}Ne. On the basis of this model, it is expected that the electric transitions of such negative-parity states to the ground state $J^\pi = \frac{1}{2}^+$ are considerably smaller than those of collective transitions, since the negative-parity band has a much different intrinsic structure from the ground-state band. Contrary to this, Litherland, Clark, and Broude[3] have observed a strong $E3$ Coulomb excitation of the 1.35-MeV $\frac{5}{2}^-$ state in ^{19}F and have suggested the importance of the octupole vibration of the ^{16}O core for this transition. This implies the inadequacy of the weak-coupling model to the ground-state transition of low-lying negative-parity states in ^{19}F. This $E3$ transition strength is only a fifth of that of the 3^- state at 6.13 MeV in ^{16}O. The remaining $E3$ strength is expected to be observed in other states.

This paper describes an experiment on electroexcitation of the low-lying states in ^{19}F. The experimental form factors for the positive-parity states are compared with those calculated on the basis of the RPC model,[22,23] where the intrinsic states of the rotational bands are formed in terms of the Nilsson model[24] extended up to principal quantum number $N=4$ with $|\Delta N|=2$ coupling. Strong excitations of negative-parity states are discussed in connection with the ^{16}O-core excitation. Figure 1 shows the band structure of ^{19}F given in Ref. 1.

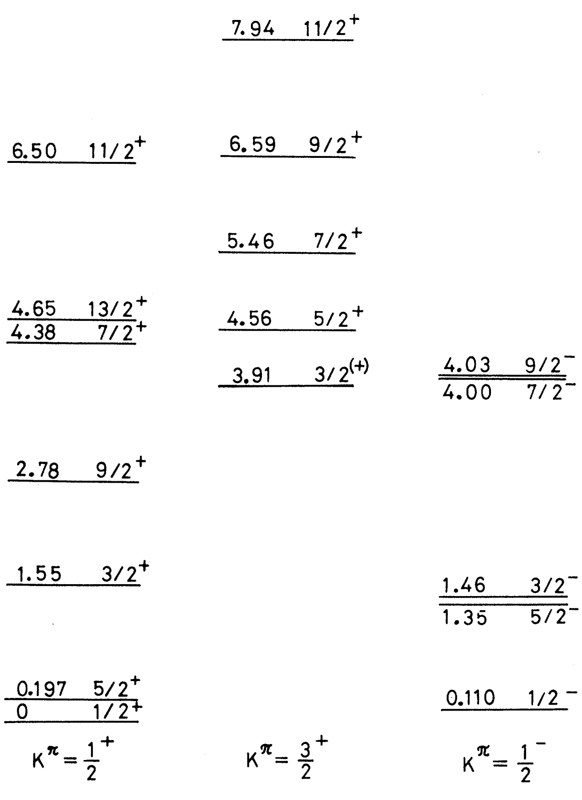

FIG. 1. Band structure of the low-lying states in ^{19}F (quoted from Ref. 1).

II. EXPERIMENTAL PROCEDURE

The experimental apparatus and technique have been described in detail elsewhere.[25] Only a simple description is given here.

The experiment was performed by using electron beams from the 300-MeV linear accelerator of Tohoku University incident on Teflon $(CF_2)_n$ targets with thicknesses of 40 and 107 mg/cm^2. In order to prevent thermal damage to the Teflon target, the average electron beam current was kept below 0.3 μA, and the target was oscillated up and down ± 1 cm with a period of 2 sec. The beam current was monitored by a secondary emission monitor and/or a Faraday cup connected to Ortec M439 current digitizers. Energy spectra of scattered electrons were measured by means of a double-focusing magnetic spectrometer (radius of central orbit = 100 cm, deflection angle = 169.7°, $n=\frac{1}{2}$, $\beta=\frac{1}{4}$) with a 33-channel solid-state-detector ladder placed at the focal plane. The over-all energy resolution was typically 0.12%. The measurements were made at laboratory scattering angles θ between 33 and 90° for incident electron total energies E_0 of 150 and 250 MeV. An energy spectrum was also measured at $E_0 = 134.5$ MeV and $\theta = 135°$ in order to extract the strength of the transverse contribution at $q_{\rm eff} = 1.28$ fm^{-1} in combination with the measurement at $E_0 = 250$ MeV and $\theta = 60°$. Peaks were found in the energy spectra at excitation energies $E_x = 0$, 0.20, 1.35, 1.55, 2.78, 4.0, 4.6, 5.4, and 5.6 MeV. A graphite target with a thickness of 106 mg/cm^2 was also used to subtract carbon components from the Teflon spectra.

The radiative correction was made for the observed spectra according to the expressions of Nguyen-Ngoc and Perez-y-Jorba,[26] and the method of Crannell.[27] Figure 2 shows the experimental spectra at momentum transfers $q = 0.87$, 1.26, and 1.62 fm^{-1}.

The absolute values of the differential scattering cross sections were derived from

$$\frac{d\sigma}{d\Omega} = \frac{Y}{CD}, \tag{1}$$

where Y is the peak area in a spectrum corrected for radiative effects, D is the time-integrated beam current, and C is a constant which includes target thickness, solid angle of a spectrometer, and efficiencies of solid-state detectors and of the current monitor. The constant C was determined from a comparison between elastic peak areas for carbon contained within the Teflon target and the well-known elastic scattering cross sections of ^{12}C over a range of $q = 0.8 \sim 1.3$ fm^{-1}. Our standardizing ^{12}C cross sections[28] correspond to a root-mean-square radius $R_{\rm rms} = 2.42$ fm. The derived ^{19}F cross sections have a 3.5% systematic error resulting from the ambiguity of the constant C.

Since the peaks at excitation energies $E_x = 1.35$ and 1.55 MeV were not observed as two isolated peaks, it was necessary to use an analysis assuming Gaussian peak shapes in order to derive areas of these two peaks separately. Figure 3 shows an example of this peak separation. In this analysis, the 1.46-MeV $\frac{3}{2}^-$ state was ignored because the observed peak appeared at 1.55 MeV in the low momentum-transfer region and at 1.35 MeV in the high momentum-transfer region; no indications were found for appearance of the 1.46-MeV state. The peak-shape analysis was also made for separation of peaks at $E_x = 0$ and 0.20 MeV, and at 5.43 and 5.63 MeV. The $E1$ component from the 0.11-MeV $\frac{1}{2}^-$ state was ignored, since this excitation was not observed in the previous electron scattering experiment.[11]

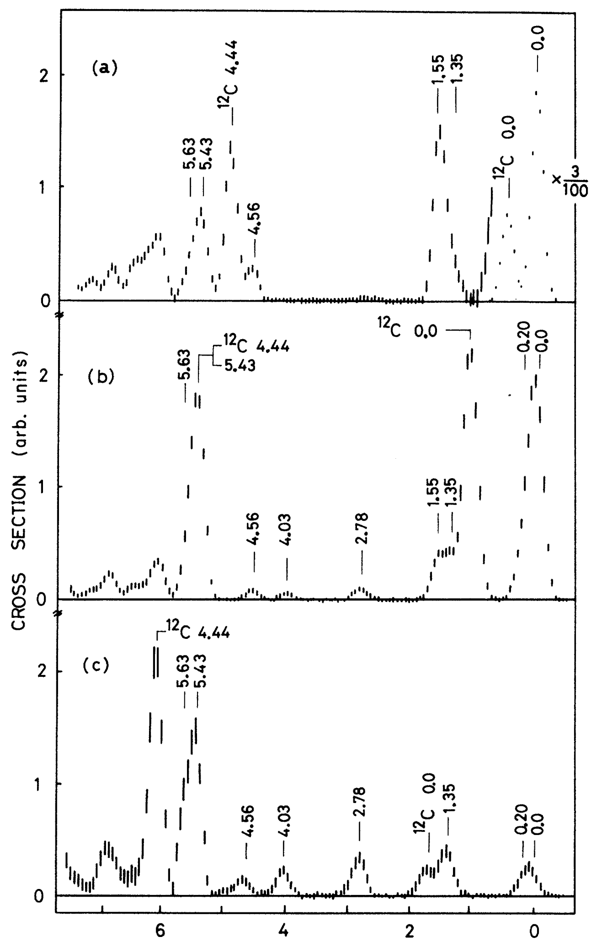

FIG. 2. Energy spectra of electrons scattered from a $(CF_2)_n$ target at the incident energy $E_0 = 250$ MeV and the scattering angles (a) $\theta = 40$, (b) 60, and (c) 80° after the radiative corrections. Adjacent three data points are averaged.

III. EXPERIMENTAL RESULTS AND DATA ANALYSIS

A. Cross section and form factor

In the first Born approximation, the electron scattering cross section is given by[29]

$$\left(\frac{d\sigma}{d\Omega}\right) = \left(\frac{d\sigma}{d\Omega}\right)_M [|F_C(q)|^2 + (\tfrac{1}{2} + \tan^2\tfrac{1}{2}\theta)|F_T(q)|^2] , \tag{2}$$

where F_C and F_T are Coulomb and transverse form factors, respectively; $(d\sigma/d\Omega)_M$ is the Mott cross section for elastic scattering from a point charge Ze with mass M_T, and is given by

$$\left(\frac{d\sigma}{d\Omega}\right)_M = \left(\frac{Ze^2}{2E_0}\right)^2 \frac{\cos^2\frac{1}{2}\theta}{\sin^4\frac{1}{2}\theta} \frac{1}{1 + (2E_0/M_T c^2)\sin^2\frac{1}{2}\theta} . \tag{3}$$

In order to take into account wavelength change of the electron in the Coulomb potential of the nucleus, the effective momentum transfer defined by[30]

$$q_{\rm eff} = q\left(1 + \frac{3Ze^2}{2E_0 R_u}\right) \tag{4}$$

is used instead of momentum transfer q throughout this paper; R_u is the equivalent-uniform radius:

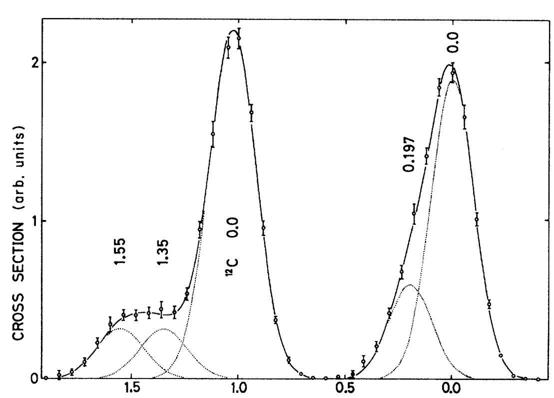

FIG. 3. An example of the separation of the overlapping peaks in the spectrum corrected for radiative effects. $E_0 = 250$ MeV, $\theta = 60°$.

TABLE I. Experimental values of total form factors for positive-parity states in ^{19}F. Errors are statistical only.

E_0 (MeV)	θ (deg)	$\|F(q,\theta)\|^2$ elastic	$\|F(q,\theta)\|^2\times 10^4$ inelastic $E_x=0.197$	$E_x=1.55$	$E_x=2.78$	$E_x=4.56$
134.5	135.0	$(4.95\pm 0.46)\times 10^{-3}$	14.9 ± 3.1	11.3 ± 3.2	8.0 ± 1.6	3.8 ± 1.3
150.0	35.0	$(5.71\pm 0.03)\times 10^{-1}$ [a]		9.1 ± 2.5		
150.0	40.0	$(4.56\pm 0.05)\times 10^{-1}$ [a]		16.9 ± 2.7		2.20 ± 1.04
150.0	45.0	$(3.88\pm 0.05)\times 10^{-1}$ [a]		17.5 ± 2.8		3.21 ± 0.77
150.0	50.0	$(3.08\pm 0.03)\times 10^{-1}$ [a]		20.0 ± 2.2		3.37 ± 0.85
150.0	55.0	$(2.46\pm 0.02)\times 10^{-1}$ [a]		25.0 ± 2.5		4.97 ± 0.93
150.0	60.0	$(1.97\pm 0.02)\times 10^{-1}$ [a]		25.3 ± 3.1		4.87 ± 0.72
150.0	70.0	$(1.01\pm 0.03)\times 10^{-1}$ [a]		28.5 ± 2.2		
250.0	33.0	$(2.26\pm 0.02)\times 10^{-1}$ [a]		24.9 ± 1.9	<0.78	5.44 ± 0.58
250.0	40.0	$(1.17\pm 0.01)\times 10^{-1}$ [a]		26.9 ± 1.4	0.94 ± 0.44	4.96 ± 0.29
250.0	50.0	$(3.01\pm 0.05)\times 10^{-2}$	29 ± 3	17.4 ± 1.3	1.59 ± 0.32	4.02 ± 0.29
250.0	60.0	$(4.85\pm 0.20)\times 10^{-3}$	17.3 ± 2.2	8.2 ± 1.2	2.80 ± 0.31	2.31 ± 0.22
250.0	70.0	$(4.86\pm 0.75)\times 10^{-4}$	4.15 ± 0.68	2.5 ± 0.9	2.83 ± 0.24	1.28 ± 0.17
250.0	80.0	$(1.47\pm 0.48)\times 10^{-4}$	1.15 ± 0.48	<0.55	2.84 ± 0.28	1.32 ± 0.18
250.0	90.0	$(2.16\pm 0.45)\times 10^{-4}$	0.97 ± 0.45	0.41 ± 0.22	2.14 ± 0.31	0.51 ± 0.18

[a] Including the 0.197-MeV state component.

$R_u^2=\frac{5}{3}\langle r^2\rangle$. All q in the formulas described below should be replaced by $q_{\rm eff}$ when making comparisons with experimental data.

The present experimental cross sections for ^{19}F are listed in Tables I and II in the unit of $(d\sigma/d\Omega)_M$. The cross section ratio $(d\sigma/d\Omega)_{\rm exp}/(d\sigma/d\Omega)_M$ is denoted by $|F(q,\theta)|^2$ and is called total form factor. The errors given in Tables I and II are standard deviations which include statistical errors arising from the peak-shape analysis and do not include systematic errors estimated to be ±3.5%.

Since the electroexcitation of collective low-lying states is caused predominantly by the Coulomb interaction, the transverse interaction may, in general, be ignored. When this is a good approximation, the experimental Coulomb form factor is simply given by

$$|F_C(q)|^2=\left(\frac{d\sigma}{d\Omega}\right)_{\rm exp}\Big/\left(\frac{d\sigma}{d\Omega}\right)_M . \qquad (5)$$

For the purpose of checking this point, Coulomb and transverse form factors at $q_{\rm eff}=1.28$ fm^{-1} were separately extracted from fitting of Eq. (2) to the data at $E_0=250$ MeV, $\theta=60°$ and at $E_0=134.5$ MeV, $\theta=135°$. It was found that transverse components

TABLE II. Experimental values of total form factors for negative-parity states in ^{19}F. Errors are statistical only.

E_0 (MeV)	θ (deg)	$\|F(q,\theta)\|^2\times 10^4$ $E_x=1.35$	$E_x=4.0$	$E_x=5.43$	$E_x=5.63$
134.5	135.0	13.8 ± 3.5	1.6 ± 0.8	16.3 ± 2.9	7.3 ± 2.8
150.0	35.0	<1.0			
150.0	40.0	<1.8			
150.0	45.0	<3.0	<0.39		
150.0	50.0	3.0 ± 1.9			
150.0	55.0	3.7 ± 1.2			
150.0	60.0	5.9 ± 2.3			
150.0	70.0	7.1 ± 1.5			
250.0	33.0	5.0 ± 1.3	<0.77	8.2 ± 1.4	2.7 ± 1.4
250.0	40.0	7.3 ± 1.1	<0.39	15.1 ± 1.0	5.1 ± 0.9
250.0	50.0	9.5 ± 1.1	0.73 ± 0.22	16.7 ± 1.6	6.8 ± 1.3
250.0	60.0	8.3 ± 1.5	1.54 ± 0.20	18.3 ± 2.1	7.7 ± 1.6
250.0	70.0	5.3 ± 1.7	1.57 ± 0.18	14.9 ± 1.6	6.7 ± 2.0
250.0	80.0	3.50 ± 0.66	1.88 ± 0.22	10.7 ± 1.1	3.7 ± 1.1
250.0	90.0	1.65 ± 0.39	1.44 ± 0.25	6.56 ± 0.75	2.19 ± 0.97

did not appreciably contribute to the cross sections at $E_0 = 250$ MeV and $\theta = 60°$, except for the case of the 2.78-MeV state.

B. Elastic scattering

The elastic scattering data were analyzed on the basis of the phase-shift calculation using the phenomenological Fermi-type charge distribution given by

$$\rho(r) = \frac{\rho_0}{1 + \exp[(r - c)/z]} . \tag{6}$$

The parameters c and z were determined as to minimize the value of χ^2 calculated for the form factors.[31] Since the experimental values of the elastic form factors in the momentum-transfer region $q < 0.9$ fm^{-1} included the inelastic components due to the 0.197-MeV state excitation, these inelastic components were subtracted using the RPC model calculation described later. The errors of c and z can be estimated from the maximum allowable value of χ^2 given by[32]

$$\chi^2 = \chi^2_{\min}\left(1 + \frac{F(1, N-p, 0.683)}{N-p}\right), \tag{7}$$

where N is the number of data points, p is the number of free parameters ($p = 2$ in the present case), and $F(\nu_1, \nu_2)$ is the statistical F distribution with degrees of freedom ν_1 and ν_2; the value of F in Eq. (7) is at confidence level 0.683, which corresponds to 1 standard deviation in the normal distribution.

In this analysis a good fit was not obtained to the data point at $E_0 = 250$ MeV and $\theta = 90°$; this data point was not used in the parameter determination. The derived values are $c = 2.58 \pm 0.04$ fm and $z = 0.567 \pm 0.013$ fm. These values are very close to those obtained by Hallowell *et al.*[11] from their electron scattering experiment. The root-mean-square radius of ^{19}F was calculated from these parameters to be $R_{\rm rms} = 2.90 \pm 0.02$ fm; this value agrees with $R_{\rm rms} = 2.885 \pm 0.015$ fm by Hallowell *et al.*[11] and with $R_{\rm rms} = 2.85 \pm 0.09$ fm derived from a μ atom experiment by Backenstoss *et al.*[33] Figure 4 shows the experimental and calculated elastic form factors.

C. Extraction of radiative transition strength

Positive-parity states

(i) 1.55-MeV $\frac{3}{2}^+$ state. The radiative $E2$ transition strength to the ground state was extracted from the experimental form factors at forward scattering angles, where the transverse component was considered to be negligibly small compared with the Coulomb form factor. In order to estimate the reduced radiative-transition strength $B(E\lambda)$, the following equation based on the Born

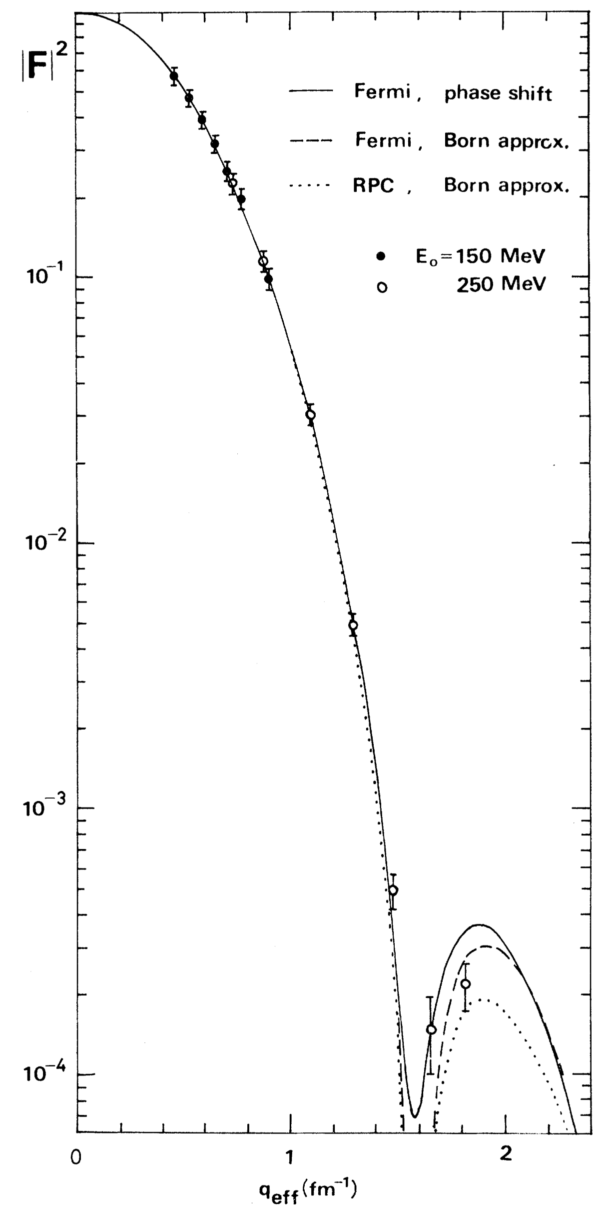

FIG. 4. Experimental and calculated elastic squared form factors for ^{19}F. The solid curve represents the C0 form factor calculated for $E_0 = 250$ MeV using the phase-shift code and the phenomenological Fermi distribution with $c = 2.58$ fm and $z = 0.567$ fm. The dashed curve is the calculation in the Born approximation for the Fermi distribution. The dotted curve denotes the theoretical form factor calculated in the RPC model (Born approximation), in which the $M1$ component is negligibly small.

TABLE III. Experimental values of electric transition strengths $J^\pi \to \frac{1}{2}^+$ (ground state).

Mode	E_x (MeV)	J^π	Present experiment $B(E\lambda,\downarrow)\ e^2\ \mathrm{fm}^{2\lambda}$ (e,e')	$\lvert M\rvert^2$	Other experiments $\lvert M\rvert^2$ (e,e')	Coul. ex.	(p,p')	(d,d')
$E2$	1.55	$\frac{3}{2}^+$	24.4 ± 3.0	8.1 ± 1.0	7.84 ± 0.67 [a] $5.89^{+0.65}_{-0.61}$ [e]	$9\ \pm3$ [b] 6.8 ± 0.7 [f]	8.4 ± 0.7 [c]	$10\ \pm3$ [d]
$E2$	4.56	$\frac{5}{2}^+$	3.1 ± 0.7	1.0 ± 0.2				
$E3$	1.35	$\frac{5}{2}^-$	$(2.4\pm0.6)\times10^2$	$11\ \pm3$	$12.4\ \pm2.5$ [a] $9.45^{+3.43}_{-2.91}$ [e]	$12\ \pm4$ [b] 7.6 ± 1.3 [f]		1.4 ± 0.6 [d]
$E3$	4.00	$\frac{7}{2}^-$	<8	<0.4				
$E3$	5.43	$\frac{7}{2}^-$	$(3.3\pm0.9)\times10^2$	$15\ \pm4$				
$E4$	2.78	$\frac{9}{2}^+$	$(9.4\pm2.0)\times10^2$	5.8 ± 1.3				
$E5$	4.03	$\frac{9}{2}^-$	$(2.0\pm0.9)\times10^4$	$16\ \pm7$				

[a] Reference 10.
[b] Reference 3.
[c] This value was calculated using the β_2 value and Eq. (7) in Ref. 7.
[d] Reference 9.
[e] Reference 11.
[f] Reference 4.

approximation has been used:

$$|F_{C\lambda}(q,J_i\to J_f)| = \frac{(4\pi)^{1/2}q^\lambda}{Ze(2\lambda+1)!!}[B(E\lambda,J_i\to J_f)]^{1/2} \times\left(1+\sum_{n=1}^{n_{\max}} a_n q^{2n}\right)\exp(-b^2q^2)\,, \tag{8}$$

where λ denotes the multipolarity of the transition; J_i and J_f are spin of the initial (ground) and final (excited) states, respectively. In the usual model-independent method,[34] the exponential factor on the right-hand side is not included; however multiplication of this factor is favorable for rapid convergence of the polynomial over a q range around the first diffraction maximum of the form factor. Equation (8) with $\lambda=2$ was fitted to the experimental form factors by the method of least squares, where $B(E2)$, a_n, and b were treated as free parameters. The maximum value of n was varied from 1 to 3, and the statistical F test[31] was carried out; sufficient goodness of fit was obtained with $n_{\max}=1$.

Another functional form of the form factor given by[35]

$$|F_{C\lambda}(q,J_i\to J_f)|^2 = \frac{4\pi B(E\lambda,J_i\to J_f)}{Z^2e^2R^{2\lambda}}[j_\lambda(qR)]^2e^{-q^2g^2} \tag{9}$$

was also used for the estimation of $B(E\lambda)$. The free parameters B, R, and g were determined by the usual χ^2-fitting procedure.[31] These two methods yielded almost the same values for the radiative transition strength and its error. The result is $B(E2,\downarrow)=24.4\pm3.0\ e^2\,\mathrm{fm}^4$ $[|M(E2)|^2=8.1\pm1.0$ W.u. (Weisskopf units)], where $B(E\lambda,\downarrow) = B(E\lambda, J_f\to J_i)$ and $B(E\lambda,\downarrow)=[(2J_i+1)/(2J_f+1)]$ $B(E\lambda,\uparrow)$. Figure 5 shows the experimental form factors and fitted curves.

(ii) 2.78-MeV $\frac{9}{2}^+$ state. It was found in this experiment that a transverse component significantly contributed to the cross section for the 2.78-MeV state at $E_0=250$ MeV and $\theta=60°$ ($q_{\mathrm{eff}}=1.28$ fm^{-1}). Therefore the fitting of Eq. (8) or (9) to the experimental total form factors is inadequate to the extraction of $B(E4)$; transverse $E4$ and/or $M5$ components should be included in the expression for fitting. In the present momentum-transfer region, transverse $E4$ and $M5$ form factors have the same q dependence and can be approximated by[36]

$$|F_{E4,M5}(q)|^2 \propto \left(\frac{\hbar q}{2Mc}j_4(qR)\right)^2 e^{-q^2g^2}\,, \tag{10}$$

where M is the proton mass. The total form factor is given by

$$|F(q,\theta)|^2 = \frac{4\pi}{Z^2e^2}\left[\frac{B(E4,\uparrow)}{R^8}+(\tfrac{1}{2}+\tan^2\tfrac{1}{2}\theta)\left(\frac{\gamma\hbar q}{2Mc}\right)^2\right] \times[j_4(qR)]^2e^{-q^2g^2}\,. \tag{11}$$

The radiative $E4$ transition strength to the ground state $B(E4,\downarrow)$ was estimated by the χ^2-fitting procedure using Eq. (11) and the experimental data, where $B(E4)$, γ, R, and g were treated as free parameters. Finally $B(E4, \downarrow) = (9.4 \pm 2.0)\times 10^2$ $e^2\,\mathrm{fm}^8$ was obtained. This transition strength corresponds to $|M(E4)|^2 = 5.8 \pm 1.3$ W.u. Figure 6 shows the experimental form factors and fitted curves for the 2.78-MeV state.

On the assumption that the transverse form factor resulted from $M5$ excitation only, $B(M5, \downarrow) = (3.0 \pm 1.2)\times 10^4$ $e^2\,\mathrm{fm}^{10}$ was also obtained using

$$B(M\lambda, \uparrow) = \left(\frac{\hbar}{2Mc}\right)^2 \frac{\lambda(2\lambda+1)^2}{\lambda+1} \gamma^2 R^{2\lambda-2} . \qquad (12)$$

According to the calculation of the ratio of $M5$ to $E4$ transverse form factors in the RPC model as described later, the subtraction of the $E4$ component from the transverse form factor yields about 15% decrease of the experimental value of $B(M5)$ presented above

(iii) 4.56-MeV $\frac{5}{2}^+$ state. Two states are known[1] at an excitation energy of 4.56 MeV: One is the $\frac{5}{2}^+$ state and the other is the $\frac{3}{2}^-$ state. The q dependence of experimental form factors indicates that the $C2$ excitation is predominant in the region of $q < 1.1\ \mathrm{fm}^{-1}$; therefore, this peak may result from the excitation of the $\frac{5}{2}^+$ state. The value of $B(E2)$ was extracted in the same manner as the case of the 1.55-MeV $\frac{3}{2}^+$ state. The result is $B(E2, \downarrow) = 3.1 \pm 0.7$ $e^2\,\mathrm{fm}^4$ $[|M(E2)|^2 = 1.0 \pm 0.2$ W.u.$]$.

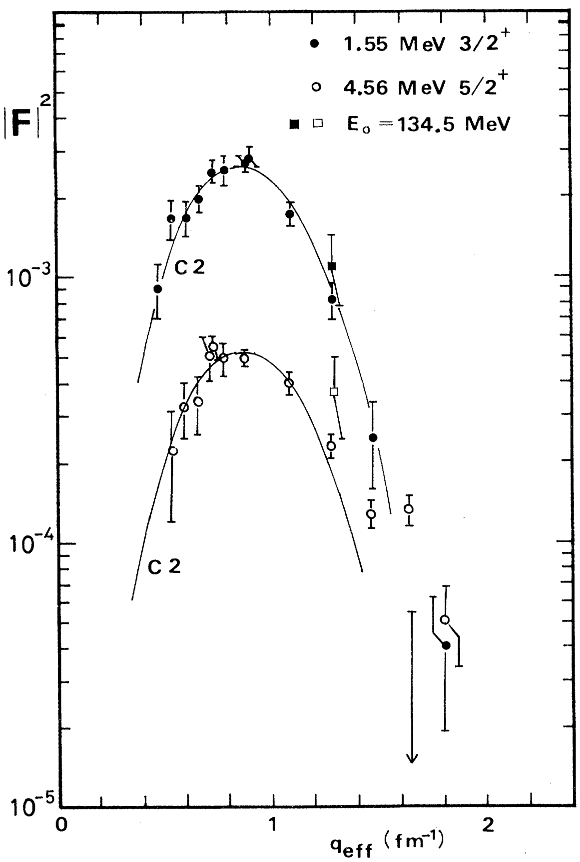

FIG. 5. Experimental squared form factors and fitted curves using Eq. (8) for the 1.55-MeV $\frac{3}{2}^+$ and 4.56-MeV $\frac{5}{2}^+$ states in ^{19}F. A vertical line with arrow at $q_{\mathrm{eff}} = 1.65$ fm^{-1} indicates the upper limit of the experimental value for the 1.55-MeV state.

Negative-parity states

(i) 1.35-MeV $\frac{5}{2}^-$ state. The radiative transition strength of the 1.35-MeV $\frac{5}{2}^-$ state to the ground state was estimated from the experimental form factors in the momentum-transfer region $q < 1.3$ fm^{-1} by the same method as the case of the 1.55-MeV state, and $B(E3, \downarrow) = (2.4 \pm 0.6)\times 10^2$ $e^2\,\mathrm{fm}^6$ was obtained. This value corresponds to $|M(E3)|^2 = 11 \pm 3$ W.u. The experimental form factors and the fitted curve are shown in Fig. 7.

(ii) 4.00-MeV $\frac{7}{2}^-$ and 4.03-MeV $\frac{9}{2}^-$ states. The peak at $E_x = 4.0$ MeV in the scattered electron energy spectra includes the 3.91-MeV $\frac{3}{2}$ ($M1$, $E2$ or $E1$, $M2$), 4.00-MeV $\frac{7}{2}^-$ ($E3$, $M4$), and 4.03-MeV $\frac{9}{2}^-$ ($M4$, $E5$) states. The shape of the peak, however, shows that the 3.91-MeV state is not the

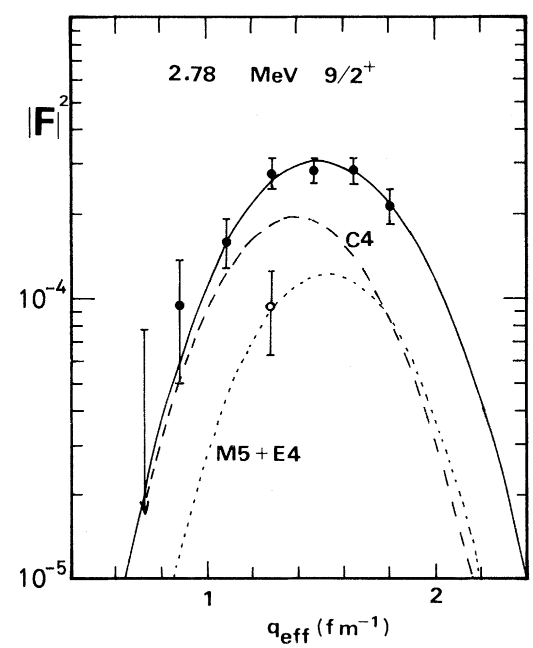

FIG. 6. Experimental squared form factors for the 2.78-MeV $\frac{9}{2}^+$ state in ^{19}F. The curves are the fitted form factors using Eq. (11). $R = 3.2$ fm, $g = 1.0$ fm. The closed circles and the solid curve represent total form factors for $E_0 = 250$ MeV; the dashed curve denotes $|F_{C4}|^2$; the open circle at $q_{\mathrm{eff}} = 1.28\ \mathrm{fm}^{-1}$ and the dotted curve are $|F_T|^2$ (transverse $E4$ and $M5$). A vertical line with arrow indicates the upper limit of the experimental total form factor at $E_0 = 250$ MeV, $\theta = 33°$.

main component; furthermore the q dependence of the form factor for this peak shows that the low multipolarity ($\lambda \leq 2$) contribution is unappreciably small. Therefore this peak can be regarded to consist of the 4.00- and 4.03-MeV states. The q dependence of the experimental form factors for this peak is explained as a composite of the $C3$ and $C5$ components. The strength of each component was estimated by fitting of Eq. (9) to experimental form factors. A parameter search for R and g was not carried out, since the number of data points was only a few. The parameters R and g were taken to be $R = 2.8 \sim 3.3$ fm and $g = 1.0$ fm, which were determined from the experimental $C2$, $C3$, and $C4$ form factors for the 1.55-, 1.35-, and 2.78-MeV states, respectively. It is seen in Fig. 8 that the 4.0-MeV peak is dominated by a $C5$ transition which results only from the 4.03-MeV $\frac{9}{2}^-$ state excitation. The reduced radiative $E5$ transition strength of this state to the ground state was estimated to be $B(E5, \downarrow) = (2.0 \pm 0.9) \times 10^4\ e^2\ \mathrm{fm}^{10}$. The value of $B(E3, \downarrow)$ of the 4.00-MeV $\frac{7}{2}^-$ state was smaller than 8 $e^2\,\mathrm{fm}^6$. In this estimation the transverse components were ignored, because the experimental value of the transverse form factor was very small at $q_{\mathrm{eff}} = 1.28\ \mathrm{fm}^{-1}$ where transverse $E3$ and $M4$ components were expected to have the maximum value.

(iii) 5.43-MeV $\frac{7}{2}^-$ and 5.63-MeV states.. A broad peak was observed at excitation energy at 5.4 MeV. This peak contains the 5.34-MeV $\frac{1}{2}$, 5.43-MeV $\frac{7}{2}^-$, 5.46-MeV $\frac{7}{2}^+$, 5.50-MeV $\frac{3}{2}^+$, 5.54-MeV $\frac{5}{2}^+$, $\frac{7}{2}^-$,

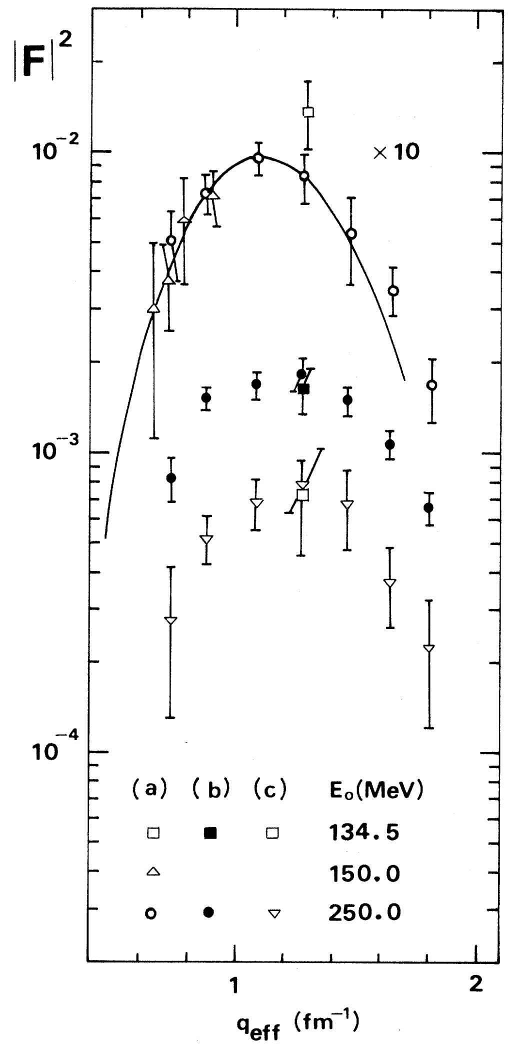

FIG. 7. Experimental squared form factors for (a) the 1.35-MeV $\frac{5}{2}^-$, (b) 5.43-MeV $\frac{7}{2}^-$, and (c) 5.63-MeV states in ^{19}F. The solid curve represents the calculated $C3$ form factor Eq. (8) fitted to the data points for the 1.35-MeV state in the region of $q < 1.3\ \mathrm{fm}^{-1}$. From this curve the value of $B(E3)$ was deduced. The values of the squared form factors for (a) are multiplied by 10 in the figure.

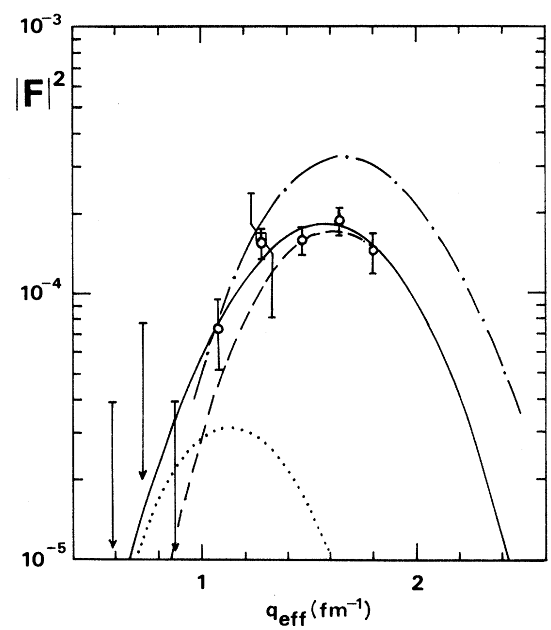

FIG. 8. Squared form factors for the 4.0-MeV peak which results from the excitations of the 4.00-MeV $\frac{7}{2}^-$ and 4.03-MeV $\frac{9}{2}^-$ states. The square denotes the data point at $E_0 = 134.5$ MeV, $\theta = 135°$. The $C3$ and $C5$ squared form factors given by Eq (9) are fitted to experimental data points and shown with the solid curve ($C3 + C5$), dotted curve ($C3$), and dashed curve ($C5$). $R = 3.2$ fm, $g = 1.0$ fm. The dash-dotted curve represents the calculated $C5$ form factor for the $1g_{9/2}1p_{1/2}{}^{-1}$ particle-hole excitation of the doubly closed ^{16}O core (harmonic oscillator model, $b = 1.85$ fm). Vertical lines with arrows indicate upper limits of the experimental form factors.

and 5.63-MeV $(\frac{1}{2}, \frac{3}{2})^-$ states.[1] The highest peak is always at 5.43 ± 0.06 MeV, and the remainder is at 5.63 ± 0.06 MeV. The form factors for these two peaks have nearly the same q dependence, which is similar to that of the $C3$ form factor for the 1.35-MeV $\frac{5}{2}^-$ state; the strength of the 5.4-MeV peak is about 2 times as large as that of the 1.35-MeV state; therefore it may be considered that the larger peak arises from the excitation of the 5.43-MeV $\frac{7}{2}^-$ state.

The ground-state $E3$ transition strength of this state was estimated from a direct comparison of experimental form factors with those for the 1.35-MeV state in the region of $q = 0.73 \sim 1.28\ \mathrm{fm}^{-1}$ because of the lack of low-q data points sufficient for a model-independent determination of $B(E3)$. The extracted value of the transition strength to the ground state is $B(E3, \downarrow) = (3.3 \pm 0.9) \times 10^2\ e^2\mathrm{fm}^6$ $[|M(E3)|^2 = 15 \pm 4\ \mathrm{W.u.}]$.

The value of $B(E3)$ of the 5.63-MeV state was also estimated in the same manner, on the assumption that the $C3$ excitation of this state was possible (i.e., $J^\pi = \frac{5}{2}^-$ or $\frac{7}{2}^-$). The value $B(E3,\ \mathrm{g.s.} \rightarrow 5.63\ \mathrm{MeV}) = (5.2 \pm 1.5) \times 10^2\ e^2\mathrm{fm}^6$ was obtained.

D. Deformation parameters

The rigid-rotor model is not a good approximation for the low-lying states in ^{19}F, especially for the $E4$ transition of the 2.78-MeV $\frac{9}{2}^+$ state, as discussed later; however, deformation parameters are convenient for comparison of the transition strengths with other experimental data such as the (p, p') reaction data obtained by de Swiniarski *et al.*[19]

On the assumption that the ground $\frac{1}{2}^+$, 1.55-MeV $\frac{3}{2}^+$, and 2.78-MeV $\frac{9}{2}^+$ states belong to the same rotational band, the surface-deformation parameters β_2 and β_4 have been extracted for the ground intrinsic state from the experimental Coulomb form factors. The $C0$, $C2$, and $C4$ form factors have been calculated in the first Born approximation using the Fermi-type charge distribution given by formula (6) in which the half density radius c was replaced with

$$c(\theta) = c[1 + \beta_2 Y_{20}(\cos\theta) + \beta_4 Y_{40}(\cos\theta)] \ . \tag{13}$$

This definition of the deformation parameters is the same as that given in Refs. 11, 19, and 37. The parameters c, z, β_2, and β_4 have been determined under the following conditions: (i) The root-mean-square radius $R_{\mathrm{rms}} = 2.89$ fm; (ii) the first diffraction minimum of the elastic form factor should appear at $q_{\mathrm{eff}} = 1.57\ \mathrm{fm}^{-1}$, and (iii) the strengths of the $C2$ and $C4$ form factors at the first diffraction maxima should fit to the experimental data. The best fit was obtained with $c = 2.60$ fm, $z = 0.527$ fm, $\beta_2 = 2.43$, and $\beta_4 = 0.12$. The present values of deformation parameters are in good agreement with those of de Swiniarski *et al.*[19] These values are summarized in Table IV with other data. Figure 9 shows the calculated and experimental form factors. The experimental points of $C4$ form factors for the 2.78-MeV state were obtained by subtraction of the transverse components, estimated in the previous section, from the total form factors, except for the point at $q_{\mathrm{eff}} = 1.28\ \mathrm{fm}^{-1}$.

As can be seen from Fig. 9, the calculated $C2$ form factor deviates from the experimental values in the region of $q \gtrsim 1.1\ \mathrm{fm}^{-1}$. Although this deviation may result from inadequacy of the assumption of the simple deformed Fermi charge distribution, these deformation parameters seem to be still suitable for comparison of transition strengths with other experimental data: Good fitting to the $C2$ and $C4$ form factors in the momentum-transfer region up to $1.4\ \mathrm{fm}^{-1}$ requires an increase of c, which does not change the present values of the deformation parameters within the estimated errors; while the calculated $C0$ form factor slightly deviates from the experimental values.

TABLE IV. Experimental values of surface-deformation parameters of the ground-state band in ^{19}F. The deformation parameters of the single-particle field based on the Nilsson model are also presented.

		β_2	β_4
Present	(e, e')	0.43 ± 0.02	0.12 ± 0.02
de Swiniarski *et al.* (Ref. 19)	(p, p')	0.44 ± 0.04	0.14 ± 0.04
Lutz *et al.* (Ref. 37)	(p, p')	0.43	$\frac{1}{3}\beta_2$ [a]
Hallowell *et al.* (Ref. 11)	(e, e')	0.41 0.48	0.17 [a] 0 [a]
single-particle field rigid rotor		0.41	0.11
RPC		0.38	0.06

[a] Assumed values.

IV. DISCUSSION

A. Comparison with the rotation-particle coupling model

The experimental form factors for positive-parity states in ^{19}F are compared with the rotational model including rotation-particle coupling (RPC) term.[22,23] The intrinsic states of the rotational bands are formed in terms of the Nilsson model.[24] It is assumed that the intrinsic states considered here consist of 16 nucleons filling the

Nilsson orbitals Nos. 1–4, two outer neutrons coupled to spin $J=0$, and an odd proton in a RPC orbital. The previous RPC calculations[12,13] based on the Nilsson model for ^{19}F have been made for the quadrupole deformation parameter $\delta \approx 0.3$, and within the principal quantum number $N=2$. However, such calculations cannot explain the strengths of the experimental $C2$ and $C4$ form factors for the ground-state band in ^{19}F. The calculated values are 10^{-1}–10^{-2} as large as the experimental values. For improvement of the theoretical $C2$ transition strength, a large value of δ or mixing of basic vectors with $N>2$ is necessary for a single-particle orbital calculation. It is favorable for the explanation of the $C4$ transition strength in the ground-state band to take into account $N>2$ mixing.

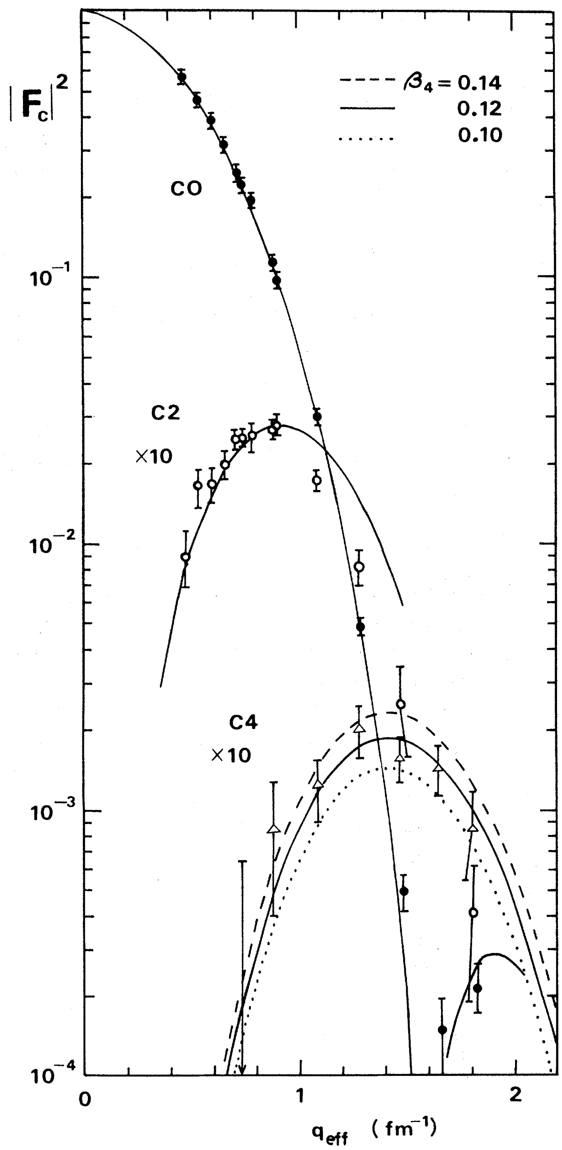

FIG. 9. The $C0$, $C2$ $(\frac{1}{2}^+ \to \frac{3}{2}^+)$, and $C4$ $(\frac{1}{2}^+ \to \frac{9}{2}^+)$ squared form factors calculated in the rigid-rotor model using the deformed Fermi distribution with $c=2.60$ fm, $z=0.527$ fm, $\beta_2=0.43$, and $\beta_4=0.12\pm0.2$. The experimental points are as follows: $C0$: the ground state (closed circles); $C2$: the 1.55-MeV state (open circles); $C4$: the 2.78-MeV state (triangles, after subtraction of the transverse component). The upper limit of the experimental $C4$ form factor at $q_{\text{eff}}=0.73$ fm^{-1} is indicated by a vertical line with arrow.

The single-particle orbitals were calculated in the truncated space with $N \leq 4$ using the formulation and the Nilsson parameters κ and μ presented by Chi.[38] The Coriolis mixing amplitudes were calculated for 21 positive-parity orbitals. The parameters used are as follows: The moment-of-inertia parameter $\hbar^2/(2\mathscr{I})=0.242$ MeV is the average value of 0.272 and 0.212 MeV which are calculated from the excitation energies of the first 2^+ and 4^+ states in ^{20}Ne, respectively; the single-particle harmonic oscillator energy $\hbar\omega=13.4$ MeV corresponds to the oscillator length parameter $b=1.76$ fm which is determined so as to reproduce the experimental value of the ^{19}F ground state root-mean-square radius $R_{\text{rms}}=2.89$ fm; the quadrupole deformation parameter was taken to be $\delta=0.32$ so as to reproduce the strength of the form factor at the first diffraction maximum for the 1.55-MeV $\frac{3}{2}^+$ state; the experimental value

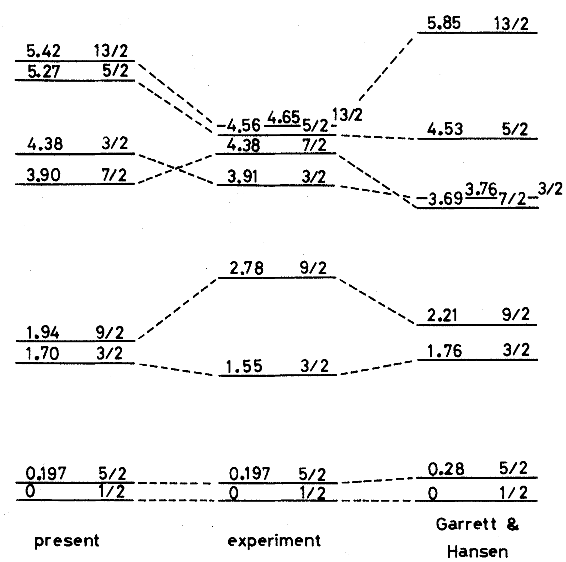

FIG. 10. Comparison of positive-parity energy-levels in ^{19}F up to 6 MeV calculated in the RPC model $(N \leq 4)$ with experiment. The previous RPC calculation $(N=2)$ by Garrett and Hansen (Ref. 13) is also presented. Parameters used in the present calculation: $\delta=0.32$, $\kappa=0.05$, $\mu=0\,(N\leq 2)$, $0.35\,(N=3)$, $0.45\,(N=4)$, $\hbar^2/2\mathscr{I}=0.242$ MeV, and $\hbar\omega=13.4$ MeV.

of the transition strength at the photon point was not used. The calculated energy levels up to 6 MeV are presented in Fig. 10 with the experimental positive-parity levels[1] and the previous result calculated within $N=2$ by Garrett and Hansen.[13] In the present calculation the lowest $\frac{5}{2}^+$, $\frac{3}{2}^+$, and $\frac{9}{2}^+$ states predominantly belong to the ground-state band; the lowest $\frac{7}{2}^+$ state has strong band mixing similar to the previous calculation by Garrett and Hansen.[13]

The radiative ground-state transition strengths of the low-lying positive-parity states were calculated using these RPC wave functions. Good agreement was obtained for the $E2$ and $E4$ transitions of the lowest $\frac{5}{2}^+$, $\frac{3}{2}^+$, and $\frac{9}{2}^+$ states. Nuclear moments of the ground $\frac{1}{2}^+$ and 0.197-MeV $\frac{5}{2}^+$ states were also calculated, where the collective gyromagnetic ratio $g_R = Z/A$ was used in the case of magnetic dipole moments.[24] These results are listed in Tables V and VI with experimental values.

Theoretical Coulomb and transverse form factors for the low-lying positive-parity states were calculated in order to compare with the experimental form factors. Figures 4, 11, and 12 show comparison between the experimental and theoretical form factors. No appreciable transverse contribution to the cross sections at forward angles was found as compared with Coulomb form factors except for the lowest $\frac{9}{2}^+$ state. The experimental form factors for the 2.78-MeV $\frac{9}{2}^+$ state was well explained with the calculated $C4$, $E4$, and $M5$ form factors, where the calculated $M5$ form factor is fairly large. It is clearly seen from Fig. 12 that the RPC is essential to the excitation of the 2.78-MeV state; the calculated form factor without RPC is considerably smaller than that with RPC. This large RPC effect means that the hexadecapole deformation of the ground intrinsic state is not so large as that derived from an analysis based on the rigid-body assumption for the experimental results of the ^{19}F(p, p') reaction.[19]

If RPC were neglected, a small hexadecapole (Y_{40}) deformation of the single-particle field would be necessary, and the deformation parameters should be $\delta = 0.33$ and $\delta_4 = 0.004$ in order to reproduce the Coulomb form factors for the 1.55- and 2.78-MeV states, where δ_4 denotes the strength of Y_{40}-deformation of the single-particle field as defined by Horikawa.[39] These parameters, however, cannot reproduce the strength of the transverse form factor F_T for the 2.78-MeV state: This calculated strength is about one-half of the experimental value. It is interesting that this value of δ is very close to that of the ground-state band in ^{20}Ne ($\delta = 0.331$) found by Horikawa[39] from an analysis of the experimental data[18] on inelastic electron scattering; the value of δ_4 in ^{19}F is 40% of that in ^{20}Ne.

Brihaye and Reidemeister[40] have given expressions for the surface-deformation parameters β_2 and β_4 of the Nilsson single-particle field as a function of δ and δ_4. The values of β_2 and β_4 at the half density radius $c = 2.60$ fm were calculated from $\delta = 0.33$ and $\delta_4 = 0.004$ according to their expressions, and found to be $\beta_2 \approx 0.41$ and $\beta_4 \approx 0.11$. These values agree with those obtained for the deformed Fermi distribution and with those derived from the (p, p') reaction.[19] This agreement may suggest that the deformation of the single-particle field used above is nearly self-consistent. In the

TABLE V. Ground-state transition strengths calculated in terms of the RPC model and those calculated using the same parameters without RPC. The present and previous experimental values are also listed.

E_x^{exp} (MeV)	J^π	Mode	$B[{}^{E\lambda}_{M\lambda}, J^\pi \to \frac{1}{2}^+ \text{ (g.s.)}]\ e^2\mathrm{fm}^{2\lambda}$ RPC	Without RPC	Experimental
0.197	$\frac{5}{2}^+_1$	$E2$	23.4	21.8	21.25 ± 0.25 [a]
		$M3$	41.8	35.9	
1.55	$\frac{3}{2}^+_1$	$M1$	1.04×10^{-3}	0.335×10^{-3}	$(1.0 \pm 0.4) \times 10^{-3}$ [b]
		$E2$	25.2	21.8	24.4 ± 3.0
2.78	$\frac{9}{2}^+_1$	$E4$	9.74×10^2	5.32×10^2	$(9.4 \pm 2.0) \times 10^2$
		$M5$	2.03×10^4	0.941×10^4	$(3.0 \pm 1.2) \times 10^4$ [c]
4.38	$\frac{7}{2}^+_1$	$M3$	0.889	0.0390	
		$E4$	1.42×10^3	5.32×10^2	
4.56	$\frac{5}{2}^+_2$	$E2$	0.272	1.54	3.1 ± 0.7
		$M3$	0.267	5.56	

[a] Reference 4.
[b] Reference 8.
[c] Assumed pure $M5$ for transverse form factors.

case of the RPC model, the surface-deformation parameters of the single-particle field are $\beta_2 \approx 0.38$ and $\beta_4 \approx 0.06$; the value of β_4 is only one-half of that in the rigid-rotor model. This decrease of β_4 value indicates that the RPC effect is important and cannot be ignored in a study of the hexadecapole deformation of ^{19}F.

It should be noted that the $C4$ excitation of the

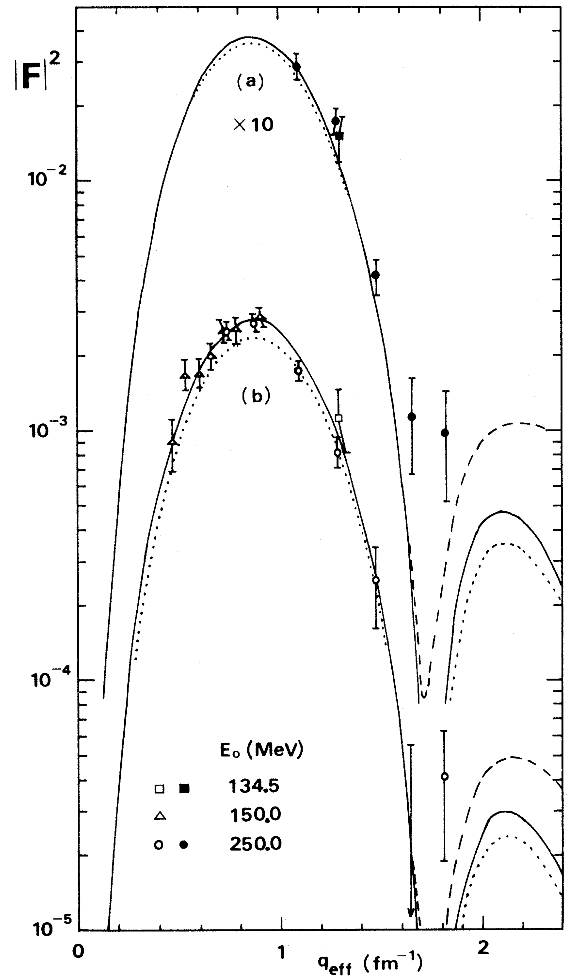

FIG. 11. Experimental and theoretical squared form factors for (a) the 0.197-MeV $\frac{5}{2}^+$ state and (b) the 1.55-MeV $\frac{3}{2}^+$ state in ^{19}F. The solid curves represent the $C2$ form factors squared, calculated in the RPC model. The dotted curves show the calculation of the $C2$ form factors squared, without RPC, using the same parameters of the single-particle field as those in the case of the RPC model. The dashed curves are the total form factors including small transverse components calculated for $E_0 = 250$ MeV. The experimental and theoretical squared form factors for (a) are multiplied by 10 in the figure. The upper limit of the experimental form factor for (b) at $q_{\rm eff} = 1.65$ fm^{-1} is indicated by a vertical line with arrow.

TABLE VI. Comparison of calculated and experimental nuclear moments for the ground state and the 0.197-MeV state in ^{19}F: Magnetic dipole moments μ in units of nuclear magnetons, and electric quadrupole moment Q in $e\,$fm^2.

E_x (MeV)	J^π		RPC	Experimental [a]
0	$\frac{1}{2}^+$	μ	2.47	2.63
0.197	$\frac{5}{2}^+$	μ	3.15	3.69 ± 0.04
		Q	−10.3	−(10 ± 2)

[a] Reference 1.

4.38-MeV $\frac{7}{2}^+$ state has not been observed in the experiment: $|F|^2 < 5 \times 10^{-5}$ in the momentum-transfer region $q = 1.3 \sim 1.6$ fm^{-1}; on the other hand, the calculated $C4$ strength is as large as that of the 2.78-MeV $\frac{9}{2}^+$ state.

The theoretical value of $B(E2, \downarrow)$ of the second $\frac{5}{2}^+$ state is nearly one-tenth as large as the experimental value of the 4.56-MeV $\frac{5}{2}^+$ state. It is found in the present RPC calculation that the theoretical form factors for the states predominantly belong-

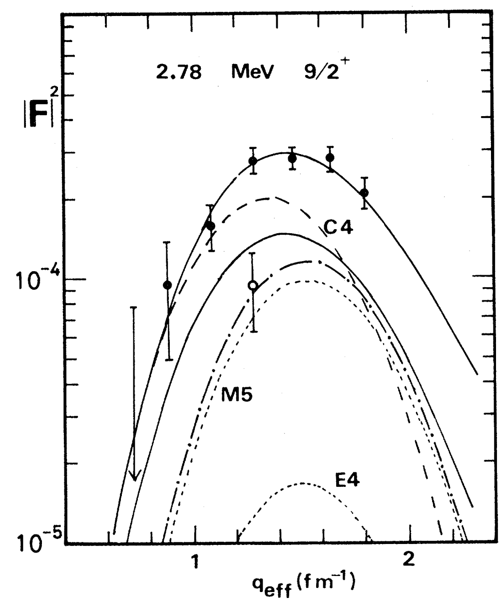

FIG. 12. Experimental and theoretical squared form factors for the 2.78-MeV $\frac{9}{2}^+$ state in ^{19}F. The curves are the theoretical values calculated in the RPC model. The closed circles and upper solid curve represent total form factors for $E_0 = 250$ MeV; the dashed curve is $C4$; the open circle and the dash-dotted curve are transverse $E4 + M5$; the dotted curves are $E4$ (lower) and $M5$ (upper). The lower solid curve shows the total form factor calculated without RPC using the same parameters as those in the RPC case ($E_0 = 250$ MeV). A vertical line with arrow indicates the upper limit of the experimental total form factor at $E_0 = 250$ MeV, $\theta = 33°$.

ing to the ground-state band are in good agreement with the experimental form factors, but good agreement is not obtained for the other states: the 4.38-MeV $\frac{7}{2}^+$ and 4.56-MeV $\frac{5}{2}^+$ states. This disagreement indicates that the excited bands of ^{19}F have more complicated configurations than those described above.

B. Comparison with the shell model

The electromagnetic properties of positive-parity states in ^{19}F have been studied in the $(sd)^3$-shell model by several authors.[14-16] The transition strength calculations in this model have been restricted to only $M1$ and $E2$ transitions, and have not been extended to transitions with the higher multipolarities: $M3$, $E4$, and $M5$. The calculated $E2$ transition strengths of the lowest $\frac{5}{2}^+$ and $\frac{3}{2}^+$ states to the ground state agree with experiment.

In comparison with the present experimental data on the ground-state transition strengths $|M(E2)|^2$, good agreement is found for the second $\frac{5}{2}^+$ state in contrast to the RPC model calculation. The theoretical values derived in the shell model are as follows: $E_x = 4.89$ MeV, $|M|^2 = 1.12$ W.u. (Benson and Flowers[14]); $E_x = 4.6$ MeV, $|M|^2 = 0.59$ W.u. (Arima, Sakakura, and Sebe[15]); $E_x = 4.97$ MeV, $|M|^2 = 0.42$ W.u. (Rogers[16]). These values are comparable with the experimental values: $E_x = 4.56$ MeV, $|M|^2 = 1.0 \pm 0.2$ W.u.

C. Negative-parity states

The observed $E3$ transition strengths are compared with the $E3$ strength of the 6.13-MeV 3^- state in ^{16}O. The comparison of the transition strengths is made for the squared Coulomb-octupole matrix element:

$$f = \frac{Z^2}{4\pi} |F(q)|^2 = \frac{1}{2J_i + 1} |\langle J_f \| M_3 \| J_i \rangle|^2 , \qquad (14)$$

instead of $B(E3)$. The values of f at the first diffraction maximum (denoted by $f_{\max}$) are as follows: $f_{\max}(^{19}\mathrm{F})/f_{\max}(^{16}\mathrm{O},\ 6.13\ \mathrm{MeV}) = 0.20$ for the 1.35-MeV $\frac{5}{2}^-$ state, 0.36 for the 5.43-MeV $\frac{7}{2}^-$ state, and 0.15 for the 5.63-MeV state (assumed $\frac{5}{2}^-$ or $\frac{7}{2}^-$). The sum of $f_{\max}$ for these three states is 71% of the $f_{\max}$ value for the 6.13-MeV 3^- state in ^{16}O; here $f_{\max}(^{16}\mathrm{O},\ 6.13\ \mathrm{MeV}) = 3.3 \times 10^{-2}$ is used.[41] The 5.43-MeV state may be regarded as the main part of the octupole vibration of the ^{16}O core in ^{19}F.

The RPC model described in the previous section was applied to the negative-parity states, but the calculation failed in explanation of energy levels and the ground-state transition strengths: The calculated values of $B(E3)$ and $B(E5)$ were too small.

The theoretical electric octupole transition strength of the 1.35-MeV $\frac{5}{2}^-$ state to the ground state has been calculated in terms of the shell model by Harvey,[42] Arima, Horiuchi, and Sebe,[21] Benson and Flowers,[14] and McGrory[43]; their values were considerably smaller than the experimental value, unless a large value of the effective charge was used compared with that adjusted to fit $B(E3)$ for ^{16}O as discussed by Dehnhard and Hintz.[9] In order to account for the strong $E3$ transition of the 1.35-MeV state, Zaikin[44] has introduced the octupole vibration of the quadrupole-deformed intrinsic state; Krappe and Wille[45] have proposed the pear-shaped deformation model including the octupole vibration; however, they have not given a satisfactory explanation to such properties as the weak-coupling ($^{15}\mathrm{N} + \alpha$) features of the low-lying negative-parity states in ^{19}F.

Kaschl *et al.*[46] have assigned spin-parity $J^\pi = \frac{1}{2}^-$ or $\frac{3}{2}^-$ to the 5.63-MeV state in ^{19}F on the basis of the angular distribution measurement of the ^{20}Ne $(d, {}^3\mathrm{He})^{19}$F reaction. If this spin-parity assignment is correct, the 5.63-MeV state is excited by the $C1$ interaction, and the form factor is expected to exhibit $C3$-like q dependence as observed in the electroexcitation of the 7.12-MeV 1^- $T=0$ state in ^{16}O.[47] In this case $f_{\max}(^{19}\mathrm{F},\ 5.63\ \mathrm{MeV})$ is about one-third of that for the 7.12-MeV state in ^{16}O. This strong non-isospin-flip $C1$ excitation of ^{16}O has been interpreted by Fujii[48] as resulting from the collective vibration in the compressible mode.

The experimental $C5$ form factors are compared with a simple calculated form factor, on the assumption that the 4.03-MeV $\frac{9}{2}^-$ state is excited by the creation of a $1p_{1/2}$ proton-hole state as expected from the weak-coupling model.[21] The dash-dotted curve in Fig. 8 is the $C5$ form factor calculated for a pure $1g_{9/2}1p_{1/2}^{-1}$ particle-hole excitation of the doubly closed ^{16}O core. The experimental value is about one-half of the calculated value. This means in the weak-coupling model that the 4^+ state of the ground-state band of ^{20}Ne necessarily includes a large $1g_{9/2}$ component. This is an improbable result. Kamimura, Matsuse, and Takada[49] have shown in the vertically truncated-subspace shell-model calculation, that the probability that all four valence particles remain in the $(2s1d, 2p1f)$ shell is 90.7% for the 4^+ state of the ground-state band of ^{20}Ne. In this case, the $1g_{9/2}$ component is less than 9%, and the calculated $C5$ form factor becomes much reduced from the experimental form factor. This may suggest that a collective Y_5-mode excitation of the ground state, as well as a Y_3-mode excitation such as proposed by Krappe and Wille,[45] is necessary for explanation of the excitation of the low-lying negative-parity states in ^{19}F, which have been interpreted in terms of the $[^{20}\mathrm{Ne}\otimes 1p_{1/2}{}^{-1}]$ weak-coupling model.

It is noteworthy that the present experimental value of $|M(E5)|^2$ is comparable with that of the 4.49-MeV 5^- state of ^{40}Ca: $|M(E5)|^2 = 16.3 \pm 4.5$ in Weisskopf units.[50] Such strong $E5$ transitions have not been observed in nuclei neighboring on ^{19}F in contrast with the $E3$ case.

V. SUMMARY

For the present experimental results of electron scattering from ^{19}F, the following remarks are given. In the data analysis based on the rotational model for the positive-parity states, it is found that the RPC is essential, in particular, to the $C4$ and $M5$ excitations of the 2.78-MeV $\frac{9}{2}^+$ state. According to the RPC model, the hexadecapole nuclear surface deformation of the ground state is considerably smaller than that based on the rigid-rotor model.

Remarkable features of the negative-parity states are as follows. Collective octupole character is found for the 1.35-MeV $\frac{5}{2}^-$ and 5.43-MeV $\frac{7}{2}^-$ states, which are compared to the octupole-vibrational state at 6.13 MeV in ^{16}O. A possibility of the collective non-isospin-flip $C1$ excitation is suggested for the strong octupole-like excitation of the 5.63-MeV state. The large $C5$ excitation strength of the 4.03-MeV $\frac{9}{2}^-$ state is comparable with that of the collective 5^- state at 4.49 MeV in ^{40}Ca.

The authors wish to thank Professor G. A. Peterson for his valuable comments on the manuscript. The support of many people at the laboratory is gratefully acknowledged.

---

*Present address: Tokyo Shibaura Electric Company, Ltd., Kawasaki, Japan.

[1] F. Ajzenberg-Selove, Nucl. Phys. A190, 1 (1972).
[2] P. H. Stelson and F. K. McGowan, Nucl. Phys. 16, 92 (1960).
[3] A. E. Litherland, M. A. Clark, and C. Broude, Phys. Lett. 3, 204 (1963).
[4] T. K. Alexander, O. Hausser, K. W. Allen, and A. E. Litherland, Can. J. Phys. 47, 2335 (1969).
[5] D. Newton, A. B. Clegg, and G. L. Salmon, Nucl. Phys. 55, 353 (1964).
[6] J. A. Becker, J. W. Olness, and D. H. Wilkinson, Phys. Rev. 155, 1089 (1967).
[7] C. M. Crawley and G. T. Garvey, Phys. Rev. 167, 1070 (1968).
[8] A. R. Poletti, J. A. Becker, and R. E. McDonald, Phys. Rev. 182, 1054 (1969).
[9] D. Dehnhard and N. M. Hintz, Phys. Rev. C 1, 460 (1970).
[10] T. Walcher and P. Strehl, Z. Phys. 232, 342 (1970).
[11] P. L. Hallowell, W. Bertozzi, J. Heisenberg, S. Kowalski, X. Maruyama, C. P. Sargent, W. Turchinetz, C. F. Williamson, S. P. Fivozinsky, J. W. Lightbody, Jr., and S. Penner, Phys. Rev. C 7, 1396 (1973).
[12] E. B. Paul, Phil. Mag. 15, 311 (1957).
[13] J. D. Garrett and O. Hansen, Nucl. Phys. A188, 139 (1972). A similar RPC calculation has been carried out by B. C. Walsh and I. M. Naqib, Nucl. Phys. A140, 571 (1970). As pointed out by Garrett and Hansen, however, their Nilsson wave function significantly differs from those appearing in other literature (Refs. 13 and 38).
[14] H. G. Benson and B. H. Flowers, Nucl. Phys. A126, 305 (1969).
[15] A. Arima, M. Sakakura, and T. Sebe, Nucl. Phys. A170, 273 (1971).
[16] D. W. O. Rogers, Nucl. Phys. A207, 465 (1973). See also the reference list in Ref. 1.
[17] R. de Swiniarski, D. Glashausser, D. L. Hendrie, J. Sherman, A. D. Bacher, and E. A. McClatchie, Phys. Rev. Lett. 23, 317 (1964).
[18] Y. Horikawa, Y. Torizuka, A. Nakada, S. Mitsunobu, Y. Kojima, and M. Kimura, Phys. Lett. 36B, 9 (1971).
[19] R. de Swiniarski, A. Genoux-Lubain, G. Bagieu, J. F. Cavaignac, D. H. Worledge, and J. Raynal, Phys. Lett. 43B, 27 (1973).
[20] R. Middleton, in *Nuclear Reactions Induced by Heavy Ions*, edited by R. Bock and W. R. Hering (North-Holland, Amsterdam, 1970), p. 263.
[21] A. Arima, H. Horiuchi, and T. Sebe, Phys. Lett. 24B, 129 (1967).
[22] A. K. Kerman, K. Dan. Vidensk. Selsk. Mat.–Fys. Medd. 30, No. 15 (1956).
[23] M. E. Bunker and C. W. Reich, Rev. Mod. Phys. 43, 348 (1971).
[24] S. G. Nilsson, K. Dan. Vidensk. Selsk. Mat.–Fys. Medd. 29, No. 16 (1955).
[25] M. Kimura *et al.*, Nucl. Instrum. Methods 95, 403 (1971).
[26] H. Nguyen-Ngoc and J. P. Perez-y-Jorba, Phys. Rev. 136, B1036 (1964).
[27] H. Crannell, Phys. Rev. 148, 1107 (1966).
[28] R. Herman and R. Hofstadter, *High-Energy Electron Scattering Tables* (Stanford U. P., Stanford, 1960).
[29] T. de Forest, Jr., and J. D. Walecka, Adv. Phys. 15, 1 (1966).
[30] D. G. Ravenhall, quoted in R. Hofstadter, Rev. Mod. Phys. 28, 214 (1956).
[31] P. R. Bevington, *Data Reduction and Error Analysis for the Physical Sciences* (McGraw-Hill, New York, 1969).
[32] W. G. Davies, quoted in N. Ensslin *et al.*, Phys. Rev. C 9, 1705 (1974).

[33]G. Backenstoss, S. Charalambus, H. Daniel, H. Koch, G. Poelz, H. Schmitt, and L. Tauscher, Phys. Lett. 25B, 547 (1967).
[34]H. Überall, *Electron Scattering from Complex Nuclei* (Academic, New York, 1971), Pt. B.
[35]R. H. Helm, Phys. Rev. 104, 1466 (1956).
[36]M. Rosen, R. Raphael, and H. Überall, Phys. Rev. 163, 927 (1967).
[37]H. F. Lutz, J. J. Wesolowski, L. F. Hansen, and S. F. Eccles, Phys. Lett. 20, 410 (1966).
[38]B. E. Chi, Nucl. Phys. 83, 97 (1966).
[39]Y. Horikawa, Prog. Theor. Phys. 47, 867 (1972).
[40]C. Brihaye and G. Reidemeister, Nucl. Phys. A100, 65 (1967).
[41]G. R. Bishop, C. Betourne, and D. B. Isabelle, Nucl. Phys. 53, 366 (1964).
[42]M. Harvey, Nucl. Phys. 52, 542 (1964).
[43]J. B. McGrory, Phys. Lett. 31B, 339 (1970).
[44]D. A. Zaikin, Nucl. Phys. 86, 638 (1966).
[45]H. J. Krappe and U. Wille, Nucl. Phys. A124, 641 (1969).
[46]G. Th. Kaschl, G. J. Wagner, G. Mairle, U. Schmidt-Rohr, and P. Turek, Nucl. Phys. A155, 417 (1970).
[47]Y. Torizuka, M. Oyamada, K. Nakahara, K. Sugiyama, Y. Kojima, T. Terasawa, K. Itoh, A. Yamaguchi, and M. Kimura, Phys. Rev. Lett. 22, 544 (1969).
[48]S. Fujii, Prog. Theor. Phys. 42, 416 (1969).
[49]M. Kamimura, T. Matsuse, and K. Takada, Prog. Theor. Phys. 47, 1537 (1972).
[50]K. Itoh, M. Oyamada, and Y. Torizuka, Phys. Rev. C 2, 2181 (1970).